Single frame image super resolution using ANFIS interpolation

Ismail, Muhammad; Yang, Jing; Shang, Changjing; Shen, Qiang

Published in:
Advances in Computational Intelligence Systems

DOI:
10.1007/978-3-030-29933-0_3

Publication date:
2019

Citation for published version (APA):
Ismail, M., Yang, J., Shang, C., & Shen, Q. (2019). Single frame image super resolution using ANFIS interpolation: An initial experiment-based approach. In Z. Ju, D. Zhou, A. Gegov, L. Yang, & C. Yang (Eds.), *Advances in Computational Intelligence Systems: Contributions Presented at the 19th UK Workshop on Computational Intelligence, 2019* (Vol. 1043, pp. 27-40). (Advances in Intelligent Systems and Computing; Vol. 1043). Springer Nature. https://doi.org/10.1007/978-3-030-29933-0_3

Single Frame Image Super Resolution using ANFIS Interpolation: An Initial Experiment-Based Approach

Muhammad Ismail[1,2], Jing Yang[1,3], Changjing Shang[1], and Qiang Shen[1]

[1] Department of Computer Science, Faculty of Business and Physical Sciences, Aberystwyth University,Aberystwyth, Ceredigion, Wales, UK
[2] Department of Computer Science, Sukkur IBA University, Sukkur, Sindh, Pakistan
[3] School of Computer Science, Nortwestern Polytechnical University, Xi'an 710072, China
{isi, jiy6, cns, qqs}@aber.ac.uk, ismail@iba-suk.edu.pk

Abstract. Image super resolution is a classical problem in image processing. Different from most of the existing super resolution algorithms that work on sufficient training data, in this work, a new super resolution method is proposed to handle the situation where the training data is insufficient by the use of ANFIS (Adaptive Network-based Fuzzy Inference System) interpolation. ANFIS interpolation aims to interpolate an effective ANFIS given only sparse data in the problem area of interest, with the assistance of two well trained ANFISs in the neighbourhood areas. The interpolated ANFIS constructs mappings from low resolution images to high resolution ones, which provides an effective mechanism for further inference of high resolution images from given low resolution ones. Experimental results indicate that the proposed approach entails improved super resolution performance for situations where there is a shortage of training data.

Keywords: Image Super Resolution, Insufficient Training Data, ANFIS Interpolation

1 Introduction

Fuzzy Inference Systems (FISs) are popular tools for reasoning with imprecise knowledge. A FIS mainly consists of a knowledge base (aka., rule base) and an inference engine. There are several types of inference engines available to implement FISs, but Mamdani [1] and TSK [2] are the two most commonly used for solving real world problems. The Mamdani inference method is more frequently used as compared to the TSK method. As far as the output of an FIS is concerned, Mamdani inference produces fuzzy outputs while TSK produces crisp ones. Thus, if the desired output is crisp whilst the Mamdani method is employed then an additional mechanism has to be applied in order to convert the output from fuzzy to crisp. However, such conversion is not required for

the outcomes produced by a TSK system, saving an additional computation procedure.

Independent of wether Mamdani or TSK inference method is used, for a problem involving sparse knowledge, no rule would be fired if a given observation does not overlap with any rule antecedent in the rule base. From knowledge acquisition perspective, this is equivalent to say that not sufficient information is available for data-driven learning of the rules to fully cover the problem domain. In order to handle such situations where sparse data is present, Fuzzy Rule Interpolation (FRI) and transfer learning techniques can be exploited.

FRI was originally proposed in [3] which could achieve appropriate conclusions using a sparse rule base, and which could also be utilised to reduce the complexity of FIS models, through manipulating neighbouring rules that do not directly match an observation. Since then, a lot of research has been done on sparse rule bases using Mamdani inference. Particularly, in [6], the scale and move based transformation technique was introduced for fuzzy interpolative reasoning. Inference was derived from two (or more) given rules that are closest to the observation to obtain the final conclusion. This method is very popular because it can achieve Normal and Convex fuzzy sets (NCF sets) in the output, provided that the relevant variables of the chosen rules are NCF sets also. A useful technique for reduction in rules was also introduced, which approximates and removes certain similar rules using the interpolated results, thereby helping to reduce computational complexity [5].

The aforementioned and almost all of the many subsequent developments (e.g., [21–28]) were however, focussed on the use of the Mamdani method until very recently. The latest approach as reported in [4] works on TSK models, by the use of a new similarity measure (that is defined on a distance factor) and also, of a tuning parameter named sensitivity factor (whose value needs to be specified with respect to different application problems given). As such, this seminal algorithm is not pure data-driven.

Inspired by this observation, a novel ANFIS [16] interpolation method has been proposed in [14], with initial evaluations using synthetic data and standard (but small scale) benchmark real-world data. The method constructs an ANFIS without requiring a large number of training data, which is very useful for situations where only sparse training data is available. It works by interpolating a group of fuzzy rules, with the assistance of two ANFISs trained in the neighbourhood of the problem area at hand. This paper further develops such work, through applying it to a much more challenging real problem, that of image super resolution where the training image pixels are insufficient. The work demonstrates the efficacy of this approach for improving the otherwise poor performance of the original ANFISs that are constructed with limited training data.

The rest of the paper is organised as follows. For academic completeness, Section 2 presents an overview of the problem of image super resolution. Section 3 details the proposed ANFIS Interpolation approach, in both descriptive and pictorial form, along with its training and testing phases. Experimental in-

vestigation is reported and discussed in Section 4, including the experimental setup, performance criteria and experimental results. Section 5 concludes the paper.

2 Single Frame Image Super Resolution

Image resolution reflects how much detail is contained in an image; an image with higher resolution means that more details are captured. High resolution (HR) images are desired in various applications, but images may only be obtained with Low Resolution (LR) due to poor image sensors, budget limitations or other practical reasons. Image Super Resolution (SR) techniques are therefore, developed to improve the resolution of LR images using computational algorithms. Typically, image SR algorithms can be divided into two classes: multi-frame image SR and single-frame image SR. Multi-frame image SR approaches [7, 8] require multiple low resolution images of the same scene, which are aligned on the sub-pixel level. Obviously, they are restricted to the situations where multiple LR images of the same scene are available. Besides, their performance greatly relies on the accuracy of the alignment algorithms. Single frame image SR methods [9, 10] are proposed to overcome the disadvantages of the multi-frame image SR approaches, generating the HR image using only one given LR image.

In single frame SR problems, the observed LR image $\mathbf{X}$ is assumed to be the down sampled version of the HR image $\mathbf{Z}$:

$$\mathbf{X} = H\mathbf{Z} \tag{1}$$

Here, H represents the down sampling operator. Single frame SR is therefore, the inverse problem of the above image degradation equation. For a given LR input $\mathbf{X}$, infinitely many LR images $\mathbf{Z}$ satisfy Eqn. (1), thus super-resolution is an extremely ill-posed inverse problem. In order to handle such a problem, other information is needed. In learning based methods [11–13], for instance, an extra database is used, consisting of a large amount of image pairs with both high and low resolutions. BAsed on such an additional database the learning algorithms learns the inverse relationships between the LR and HR images. This leads to the state of the art results in addressing single frame SR problems.

As the the machine learning techniques are developing, various learning based SR methods have been proposed, including a range of techniques capable of producing learned mappings that simulate the underlying relationship between the LR and HR images. In particular, linear mappings [11] were proposed to describe such mapping relationship. Whilst it is very simple to implement, such a method suffers from inaccurate mapping results. This raises the requirement of developing more accurate, non-linear mappings. In the literature, non-linear mappings learned by fuzzy rules [12] or deep convolutional neural networks [13] are the most commonly applied. Amongst the existing techniques, the image SR method as reported in [15] is of direct relevance to this work, which learns the non-linear mappings using an adaptive network based fuzzy inference system (ANFIS).

3 Proposed Approach

In this section a novel approach for image SR is proposed using ANFIS interpolation. The description is divided into two parts: training phase and testing phase. In the first phase, although a large number of LR-HR pixel pairs are fed into the learning system in general, for certain mapping properties there is a lack of sufficient training data (and hence, the need for interpolation). In the second part, LR images are fed to a learned ANFIS to compute the corresponding mapped HR image. Thus, it is the first phase that is scientifically more challenging.

3.1 Training Phase using ANFIS Interpolation

The proposed training process is summarised in Algorithm 3.1, while its flowchart is shown in Fig. 1. Suppose that to train an ANFIS model, 75 Bitmap images are used as the training set. LR-HR patch pairs of a size of 9 by 9 are extracted from the training data set. Then they are converted into LR-HR pixel vector pairs P. Based on their respective pixel values, P is partitioned into three subsequent categories 'small' pixels, 'medium' pixels and 'large' pixels, as depicted in the upper half of Fig. 1.

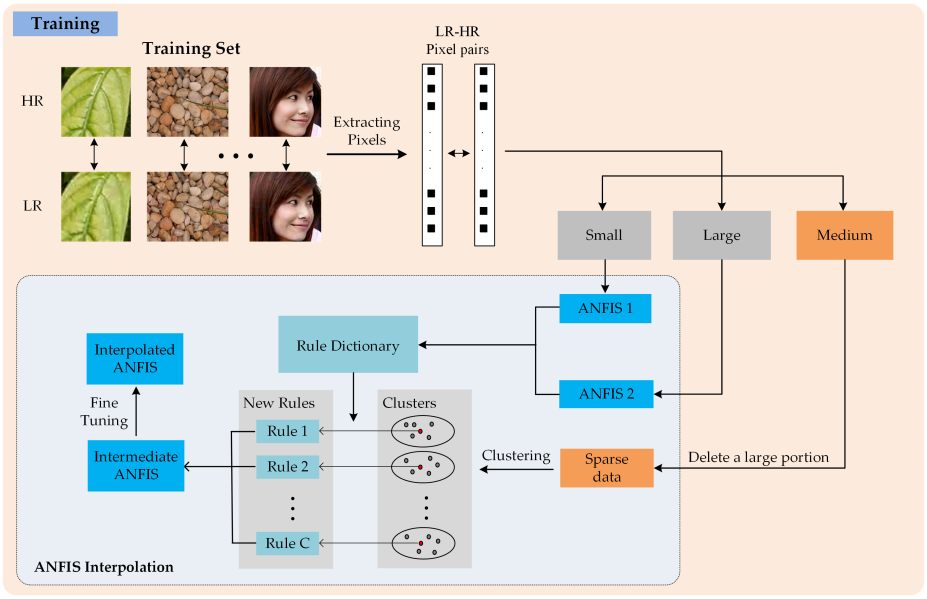

Fig. 1. Flowchart of proposed training phase.

Suppose that the 'large' and 'small' pixels in the training set are of sufficient amounts, while the 'medium' pixels are insufficient. From this, for the 'small' and 'large' pixels, two ANFISs (denoted as $\mathcal{A}_s$ and $\mathcal{A}_l$) can be trained using the standard ANFIS training procedure. However, the shortage of 'medium' pixels

will lead to very poor performance if the same ANFIS training process is directly applied. In order to improve the accuracy of the learned ANFIS under sparse training data situations, this work proposes an ANFIS interpolation mechanism to construct the required ANFIS $\mathcal{A}_m$ for the sparse 'medium' pixels. That is, the proposed ANFIS interpolation approach utilises the two well trained ANFISs $\mathcal{A}_s$ and $\mathcal{A}_l$ as source ANFISs to support the generation of a target ANFIS $\mathcal{A}_m$. This training process is detailed in the following subsections.

1) Generating a rule dictionary. A rule dictionary is constructed firstly to store the extracted fuzzy rules from the learned source ANFISs $\mathcal{A}_s$ and $\mathcal{A}_l$, which is to be subsequently used for generating an intermediate ANFIS. From a given ANFIS, a set of fuzzy production rules can be extracted. For the present application of image SR, it may be assumed that the ith rule can be expressed in the following format:

$$R_i : if\ x\ is\ A_i,\ then\ z_i = p_i x + r_i \tag{2}$$

where x denotes the input LR pixel, A_i is the corresponding fuzzy set value of the pixel, z_i represents the output of the ith rule (which contributes to the final outcome of the HR image being constructed), and r_i is a constant coefficient within the linear combination of the rule consequent.

The rule dictionary $D = \{D_a, D_c\}$ is generated by reorganising the above extracted fuzzy rules, with the antecedent part D_a and the consequent part D_c each collecting all the antecedents and consequents of those rules. Suppose that two source ANFISs consist of n_1 and n_2 rules, respectively, then there will be totally $N = n_1 + n_2$ rules in the rule dictionary. Thus, D_a consists of the antecedent parts of all the rules:

$$D_a = \{A_1\ A_2\ \cdots\ A_N\} \tag{3}$$

and the consequent part D_c consists of the consequents of the rules:

$$D_c = \begin{bmatrix} p_1 & p_2 & \cdots & p_N \\ r_1 & r_2 & \cdots & r_N \end{bmatrix} \tag{4}$$

where each column denotes the linear coefficients in the consequent part of a certain rule.

2) Interpolating an intermediate ANFIS. Having obtained the above rule dictionary, the small number of 'medium' pixel pairs $\{(x, z)\}$ are divided into C clusters using the K-means algorithm (although if preferred, any other numeric value-based clustering method may be used as the alternative to perform clustering). For the centre of each cluster, a new fuzzy rule is interpolated. Then, by aggregating all interpolated rules, an intermediate ANFIS results [15].

For each cluster C_k, compute its centre, resulting in $c^{(k)}$. Given the previously obtained antecedent part rule dictionary D_a, the first step then, is to select

K closest rule antecedent $A^i \in D_a, i = 1, \ldots, K$ with respect to $c^{(k)}$. This is done on the basis of a distance metric, say for simplicity, $d^i = d(A^i, c^{(k)}) = |Rep(A^i) - c^{(k)}|$, where $Rep(A^i)$ stands for the representative value of the fuzzy set A^i [6]. The K rule antecedents $\{A^i\}$ with the smallest distances d^i are chosen, whose index set is denoted by $\mathcal{K}$.

From this, the next step is set to find the best reconstruction weights for the chosen closest rules. This is achieved by solving the following optimisation problem under the constraint that the sum of all the weights equals to 1:

$$w^{(k)} = \min_{w^{(k)}} ||c^{(k)} - \sum_{i \in \mathcal{K}} Rep(A^i) w_i^{(k)}||^2, \ s.t. \ \sum_{i \in \mathcal{K}} w_i^{(k)} = 1 \tag{5}$$

where $w_i^{(k)}$ denotes the relative weighting of A^i. The solution of this constrained least square problem is as follows:

$$w^{(k)} = \frac{G^{-1}\mathbf{1}}{\mathbf{1}^T G^{-1}\mathbf{1}} \tag{6}$$

where $G = (c^{(k)}\mathbf{1}^T - Y)^T (c^{(k)}\mathbf{1}^T - Y)$ is a defined Gram matrix, $\mathbf{1}$ is a column vector of ones, and the columns of Y are the selected rule antecedents.

Following the standard fuzzy rule interpolation technique as per [6], the weights $w^{(k)}$ are applied onto both the antecedent part and the consequent part in interpolating a new rule to summarise the kth cluster:

$$R_k : if \ x \ is \ A^k, \ then \ z_k = p_k x + r_k \tag{7}$$

where the parameters are generated by:

$$A^k = \sum_{i \in \mathcal{K}} w_i^{(k)} A^i, \ p_k = \sum_{i \in \mathcal{K}} w_i^{(k)} p_i, \ r_k = \sum_{i \in \mathcal{K}} w_i^{(k)} r_i \ k = 1, 2, \cdots, C. \tag{8}$$

3.2 Testing Phase

The phase run to test the implemented approach is illustrated in Fig. 2. From left to right in this figure, bicubic interpolation is applied on the input LR image by the scale factor s to make an image of a larger size.

As the proposed ANFIS model works on raw pixel values LR pixels are extracted from the enlarged image and partitioned into 3 categories based on their pixel values: 'small', 'medium' and 'large'. The testing process runs through the three corresponding trained ANFISs: ANFIS $\mathcal{A}_s$, ANFIS $\mathcal{A}_l$ and the interpolated ANFIS $\mathcal{A}_m$. Those 'small' and 'large' pixel values are fed into $\mathcal{A}_s$ and $\mathcal{A}_l$ respectively while $\mathcal{A}_m$ gets those in the 'medium' range of pixel values. Thus, the trained ANFIS-based Inference takes LR pixel values as input and converts them into HR pixel values, which are subsequently converted into the required HR image. This testing phase is presented in Algorithm 3.2.

With regard to different types of image pixels, three domains are defined: Source Domain 1, Source Domain 2 and Target Domain. As indicated previously,

Algorithm 1: Training Phase using ANFIS Interpolation

Input:

1. HR natural image data set $\{\mathbf{Z}^h\}$
2. Scale factor s

Step 1: Generating Database

1. Generate LR images $\{\mathbf{X}^l\}$ from $\{\mathbf{Z}^h\}$ by rate of s;
2. Extract pixels from LR-HR image pairs $\{(\mathbf{X}^l, \mathbf{Z}^h)\}$ to form pixel vector pairs $\mathbf{P} = (\mathbf{x}, \mathbf{z})$;
3. Divide pixel pairs $\mathbf{P}$ into 'small' pixels, 'medium' pixels and 'large' pixels using K-Means algorithm;

Step 2: Training ANFIS for 'small' and 'large' pixels with standard ANFIS training procedure

1. Train first ANFIS $\mathcal{A}_\mathbf{s}$ using 'small' pixels;
2. Train second ANFIS $\mathcal{A}_\mathbf{l}$ using 'large' pixels;

Step 3: Interpolating ANFIS for 'medium' pixels

1. Construct rule dictionary by extracting rules from $\mathcal{A}_\mathbf{s}$ and $\mathcal{A}_\mathbf{l}$;
2. Construct intermediate ANFIS $\mathcal{A}_\mathbf{m}$ for 'medium' pixels by interpolating rules using $\mathcal{A}_\mathbf{s}$ and $\mathcal{A}_\mathbf{l}$;
3. Fine tune intermediate ANFIS $\mathcal{A}_\mathbf{m}$

Output:

Three learned ANFISs $\mathcal{A}_\mathbf{s}$, $\mathcal{A}_\mathbf{m}$ and $\mathcal{A}_\mathbf{l}$

Algorithm 2: Testing Phase

Input:

1. Low resolution image $\mathbf{X}$
2. Scale factor s

1. Pre-processing: Upscale LR image $\mathbf{X}$ by scale factor s using bicubic interpolation;
2. **for** each pixel of upscaled LR image:
   1) Determine type of current pixel ('small', 'medium' or 'large');
   2) Inference using corresponding ANFIS ($\mathcal{A}_\mathbf{s}$, $\mathcal{A}_\mathbf{m}$ and $\mathcal{A}_\mathbf{l}$);
   end for
3. Integrate HR pixels to form HR image $\mathbf{Z}^0$;
4. Post-processing: Apply iterative back projection: $\mathbf{Z}^{t+1} = \mathbf{Z}^t + \lambda * I(\mathbf{X} - D(\mathbf{Z}^t))$

Output:

Estimated high resolution image $\hat{\mathbf{Z}}$

the source domains contain 'small' and 'large' vectors respectively, whilst Target Domain comprises sparse 'medium' pixel vectors.

For comparative analysis purpose, three models are employed, namely: Model 1, Model 2 and Model 3, as illustrated in Table 1. These models run over the same source domain 1 and source domain 2 but a different target domain, which is to be identified. Model 1, which is an ideal (reference) model, performs ANFIS

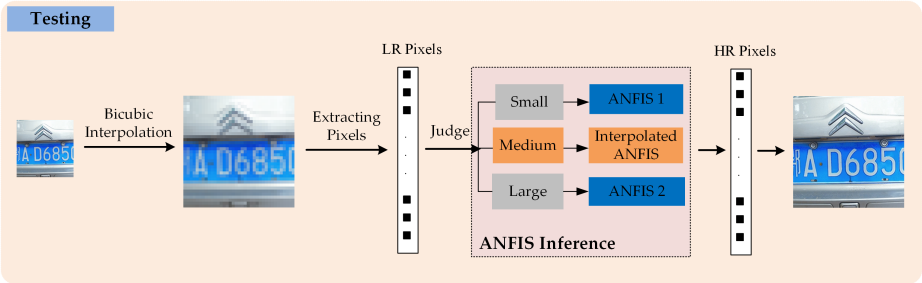

Fig. 2. Flowchart of testing phase.

Table 1. Model specification

Models	Target Domain	Interpolation	Source Domain 1	Source Domain 2
Model 1 (Reference Model)	Whole Data	No	Small Pixels	Large Pixels
Model 2	Sparse Data	No	Small Pixels	Large Pixels
Model 3 (Proposed Model)	Sparse Data	Yes	Small Pixels	Large Pixels

using whole data in the target domain with no need to apply any interpolation technique. Model 2 performs ANFIS without interpolation with the sparse data in the target domain. However, Model 3 which implements the proposed approach, runs ANFIS with interpolation over the target domain involving sparse data only. For clarity, the three models can be conceptually organised with respect to the given target data as shown in Fig. 3.

4 Experimental Results

This section presents and discusses the results of experimental comparison.

4.1 Experimental Setup

The number of images used for training and testing are 75 and 5 respectively. During the training phase, HR images are down sampled using the scale factor s to generate their respective LR images using the same factor s. Note that this scale factor s is an important input parameter as per Algorithm 3.1. In this initial experimental investigation, its value is empirically set to 2 or 3, dividing the experiments into two cases as shown in Table 2 and Table 3 respectively.

Note that the present work is developed for situations with sparse image training data, especially for the cases where in the target domain a large number

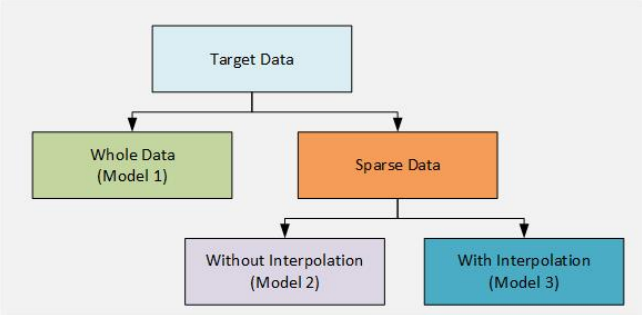

Fig. 3. Target data for learning source and target models.

of training data is missing whilst sufficient training data in neighbourhood source domains are available. Such cases can be common in different data sets. However, in this experimental investigation, in order to have ground truth to compare the performances of different approaches, for the target domain a large portion of 'medium' pixels are randomly removed to artificially create a sparse data.

4.2 Performance Criteria

The PSNR and SSIM indices are employed to quantitatively evaluate the performance of the three models.

The PSNR (Peak Signal-to-Noise Ratio) index assesses the model results by computing the difference between the ground truth HR image $\mathbf{Z}$ and the estimated HR image $\hat{\mathbf{Z}}$, which is calculated as follows:

$$MSE = \frac{\| \mathbf{Z} - \hat{\mathbf{Z}} \|_F^2}{MN} \tag{9}$$

$$PSNR = 10 \log_{10}(\frac{255^2}{MSE}) \tag{10}$$

where M, N are the image length and image width respectively, and $\| \cdot \|_F$ stands for the Frobenius norm of matrix.

The SSIM (Structure SIMilarity) index reflects the degree of structural similarity between the ground truth HR image and the estimated HR image. SSIM is defined by the following:

$$SSIM = \frac{4\mu_{\mathbf{Z}}\mu_{\hat{\mathbf{Z}}}\sigma_{\mathbf{Z},\hat{\mathbf{Z}}}}{(\mu_{\mathbf{Z}}^2 + \mu_{\hat{\mathbf{Z}}}^2)(\sigma_{\mathbf{Z}}^2 + \sigma_{\hat{\mathbf{Z}}}^2)} \tag{11}$$

with $\mu_{\mathbf{Z}}$ and $\mu_{\hat{\mathbf{Z}}}$ denote the mean value of the ground truth and that of the estimated HR image, respectively; $\sigma_{\mathbf{Z}}$ and $\sigma_{\hat{\mathbf{Z}}}$ denote their corresponding standard deviations; and $\sigma_{\mathbf{Z},\hat{\mathbf{Z}}}$ is the covariance of $\mathbf{Z}$ and $\hat{\mathbf{Z}}$. The range of the SSIM index is [0, 1]. Generally, a lager PSNR or SSIM means a better result.

4.3 Results and Discussion

Again, experimental results for cases where the scale factor is 2 and 3 are shown in Table 2 and Table 3 respectively.

Table 2. Results of three models with scale factor being 2

Image	**Index**	**Models**		
		Model 1	**Model 2**	**Model 3**
Child	PSNR (dB)	35.185954	34.549028	34.859207
	SSIM	0.948380	0.940307	0.944521
Butterfly	PSNR (dB)	28.543521	28.329785	28.417484
	SSIM	0.927894	0.919854	0.924624
Hat	PSNR (dB)	32.483129	32.144308	32.288645
	SSIM	0.910367	0.888009	0.901671
House	PSNR (dB)	32.652422	32.438947	32.599810
	SSIM	0.914100	0.896402	0.908422
Airplane	PSNR (dB)	30.798012	30.630707	30.706750
	SSIM	0.940617	0.936547	0.938622
Average	PSNR (dB)	32.20482	31.85075	32.02619
	SSIM	0.927403	0.914022	0.921915

To support analysing and comparing the performances of the three trained ANFIS models, five popular LR images (Child, Butterfly, Hat, House, and Airplane) are used. Generally speaking, the results of using scale factor of 2 are much better than those of 3. In particular, the average values of PSNR with the scale factor being 2 are 3.5 dB up to 4.2 dB higher than those with the scale factor being 3, and the average SSIM values with scale factor 2 are 0.086 up to 0.11 higher than those with scale factor 3.

Importantly, the differences in the average values of PSNR and SSIM between Model 1 (the reference) and Model 3 (the proposed approach) are approximately 0.11 dB and -0.002, respectively. This implies that the values of Model 3 are very similar to those of the reference model. Particularly, the results given in Table 2 (with scale factor being 2) indicate that the difference of average PSNR values between Model 1 and Model 3 is 0.179 dB, and that the difference of average SSIM values between these two models is only 0.0055 dB. Both differences are very minor. However, the difference between Model 2 and Model 1 is 0.354 dB which is much higher than 0.179 (of the difference between Models 1 and 3). Examining the results more closely, it can be seen that the SSIM values of Model 2 in relation to Model 1 are particularly lower for the Hat and House images as compared to the respective values of Model 3.

Table 3. Results of three models with scale factor being 3

Image	**Index**	**Models**		
		Model 1	**Model 2**	**Model 3**
Child	PSNR (dB)	30.148883	28.215039	30.052112
	SSIM	0.848713	0.803725	0.845844
Butterfly	PSNR (dB)	24.523254	23.792907	24.448903
	SSIM	0.819721	0.785855	0.815197
Hat	PSNR (dB)	29.483312	28.934074	29.403986
	SSIM	0.827285	0.798796	0.817777
House	PSNR (dB)	29.919447	29.246447	29.852731
	SSIM	0.857977	0.831277	0.845281
Airplane	PSNR (dB)	27.503117	27.093622	27.440101
	SSIM	0.864328	0.851714	0.861372
Average	PSNR (dB)	28.6136	27.65687	28.52663
	SSIM	0.841701	0.80776	0.834235

The trend of results as shown in Table 3 with the scale factor being 3 is similar. The difference of average PSNR values between Model 1 (the reference model) and Model 3 (the proposed model) is merely 0.087 dB, and the difference of average SSIM values between them is 0.0075 which is again quite similar, as with the case when the scale factor is 2. Nevertheless, the difference of average PSNR values between Model 2 and Model 1 is 0.957 dB, which is much higher than 0.087. This is also reflected by the comparatively much higher difference of 0.87 dB, regarding the same performance index between Model 3 and Model 2. As a matter of fact, the individual SSIM values of different images such as Child, Butterfly and Hat of Model 2 are quite lower than their respective values between Models 1 and 3.

As an example for qualitative illustration, Fig. 4 and Fig. 5 show the LR images of Hat and Child and their respective HR output images through running all three models, when the scare factors are 2 and 3 respectively. For comparison purpose, one patch is taken from the Hat images as given in Fig. 6 and two different patches are extracted from the Child image as shown in Fig. 7. It can be observed from these figures that in the estimated HR images using Model 2, there are obvious noise and bad edges, whilst the results of the proposed model (Model 3) are much closer the reference model (Model 1). This demonstrates that the proposed interpolated ANFIS model significantly improves over the poor performance of Model 2 that is directly trained with insufficient data.

Fig. 4. LR to HR output images of Hat when scale factor is 2.

Fig. 5. LR to HR output images of Child when scale factor is 3.

Fig. 6. Detailed HR images of Hat – From left to right: original HR image used as ground truth; estimated HR image using Model 1; estimated HR image using Model 2; estimated HR image using Model 3.

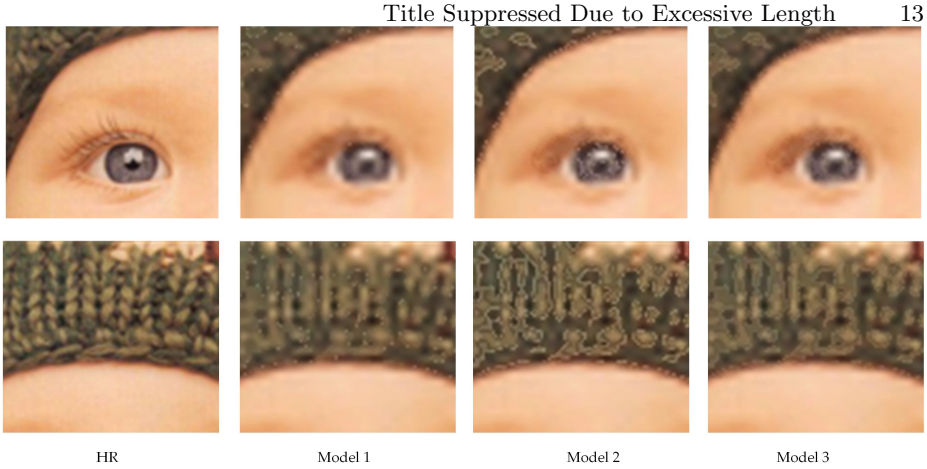

Fig. 7. Detailed HR images of Child – From left to right: original HR image used as ground truth; estimated HR image using Model 1; estimated HR image using Model 2; estimated HR image using Model 3.

5 Conclusion

This paper has offered a novel approach for single frame image super resolution, via generating ANFISs through rule interpolation. It is developed for situations with sparse image training data. The approach works at the pixel level, by dividing given low resolution image pixels into categories which are referred to as source domains, where sufficient training data are available, or target domains, where a large number of training data is missing. Then, the ANFIS in a target domain is learned through interpolating the ANFISs trained with data from its closest neighbourhood source domains. This study extends the prior work of [14] which considered sparse numerical function approximation only, and that of [15] where multiple ANFISs were mapped with the patches of an LR image to obtain the final HR image. The performance of the proposed approach has been compared to the reference model which is fed with original data, showing that it provides similar results as those attainable by the reference model while significantly improves upon the outcomes achievable by the ANFISs directly trained with sparse data without interpolation.

As an initial attempt on the development of an ANFIS-based image super resolution mechanism, and also for simplicity, the proposed approach directly works on raw image pixels. However, much research has shown that image features are usually more representative than raw image pixels. Therefore, it would be potentially beneficial to replace images' pixels with extracted features instead as input variables of the ANFISs, in an effort to strengthen the effectiveness of this work. Furthermore, as widely recognised in the literature, the use of less but more informative features may do better than utilising all extracted features [18], integrating feature selection techniques (e.g., [19, 20]) into such further developments may boost their efficiency.

6 Acknowledgment

The authors are grateful to Sukkur IBA University & Higher Education Commission, Pakistan, Aberystwyth University, UK and Northwestern Polytechnical University, China for their support in this research.

References

1. Mamdani, E. H. Application of fuzzy logic to approximate reasoning using linguistic synthesis. in Proceedings of the sixth international symposium on Multiple-valued logic 196-202 (IEEE Computer Society Press, 1976).
2. Takagi, T., Sugeno, M. Fuzzy identification of systems and its applications to modeling and control. IEEE Transactions on Systems, Man, and Cybernetics 1-132 (1985).
3. Kóczy, L., Hirota, K. Approximate reasoning by linear rule interpolation and general approximation. International Journal of Approximate Reasoning 9, 197-225 (1993).
4. Li, J., Qu, Y., Shum, H. P., Yang, L. TSK inference with sparse rule bases. in Advances in Computational Intelligence Systems 107-123 (Springer, 2017).
5. Huang, Z., Shen, Q. Fuzzy interpolation and extrapolation: A practical approach. IEEE Transactions on Fuzzy Systems 16, 13-28 (2008).
6. Huang, Z., Shen, Q. Fuzzy interpolative reasoning via scale and move transformations. IEEE Transactions on Fuzzy Systems 14, 340-359 (2006).
7. Li, X., Hu, Y., Gao, X., Tao, D., Ning, B. A multi-frame image super-resolution method. Signal Processing. 90(2), 405-414 (2010).
8. Irani, M., and Peleg, S. Super resolution from image sequences. in 10th International Conference on Pattern Recognition 115-120 (IEEE, 1990).
9. Yang, J., Wright, J., Huang, T. S., Ma, Y. Image super-resolution via sparse representation. IEEE transactions on image processing 19(11), 2861-2873 (2010).
10. Irani, D. G. S. B. M. Super-resolution from a single image. In Proceedings of the IEEE International Conference on Computer Vision 349-356 (IEEE 2009).
11. Zhang, K., Tao, D., Gao, X., Li, X., Xiong, Z. Learning multiple linear mappings for efficient single image super-resolution. IEEE Transactions on Image Processing 24(3), 846-861 (2015).
12. Purkait, P., Pal, N. R., Chanda, B. A fuzzy-rule-based approach for single frame super resolution. IEEE Transactions on Image processing 23(5), 2277-2290 (2014).
13. Dong, C., Loy, C. C., He, K., & Tang, X. Image super-resolution using deep convolutional networks. IEEE transactions on pattern analysis and machine intelligence, 38(2), 295-307 (2015).
14. Yang, J., Shang, C., Li, Y., Li, F., Shen, Q. Generating ANFISs Through Rule Interpolation: An Initial Investigation. in UK Workshop on Computational Intelligence 150-162 (Springer, 2018).
15. Yang, J., Shang, C., Li, Y., Shen, Q. Single frame image super resolution via learning multiple ANFIS mappings. in 2017 IEEE International Conference on Fuzzy Systems (FUZZ-IEEE) 1-6 (2017).
16. Jang, J.-S. ANFIS: adaptive-network-based fuzzy inference system. IEEE transactions on systems, man, and cybernetics 23, 665-685 (1993).
17. Li, F., Shang, C., Li, Y., Yang, J., Shen, Q. Fuzzy Rule Based Interpolative Reasoning Supported by Attribute Ranking. IEEE Transactions on Fuzzy Systems 26, 2758-2773 (2018).

18. Jensen, R., Shen, Q. Are more features better? EEE Transactions on Fuzzy Systems 17(6), 1456-1458 (2009).
19. Diao, R., Shen, Q. Two new approaches to feature selection with harmony search. in 2010 IEEE International Conference on Fuzzy Systems (FUZZ-IEEE) 1-7 (2010).
20. Jensen, R., Tuson, A., Shen, Q. Finding rough and fuzzy-rough set reducts with SAT. Information Sciences 255, 100-120 (2014).
21. Chen, C., MacParthalain, N., Li, Y., Price, P., Quek, C., Shen, Q.. Rough-fuzzy rule interpolation. Information Sciences 351, 1-17 (2016).
22. Chen, S., Ko, Y. Fuzzy interpolative reasoning for sparse fuzzy rule-based systems based on ?-cuts and transformations techniques. IEEE Transactions on Fuzzy Systems 16(6) ,1626-1648 (2008).
23. Chen, S., Ko, Y., Chang, Y., Pan, J. Weighted fuzzy interpolative reasoning based on weighted increment transformation and weighted ratio transformation techniques. IEEE Transactions on Fuzzy Systems 17(6), 1412-1427 (2009).
24. Yang, L., Shen, Q. Adaptive fuzzy interpolation. IEEE Transactions on Fuzzy Systems 19(6), 1107-1126 (2011).
25. Yang, L., Shen, Q. Closed form fuzzy interpolation. Fuzzy Sets and Systems 225, 1-22 (2013).
26. Chen, S., Chang, Y., Pan, J. Fuzzy rules interpolation for sparse fuzzy rule-based systems based on interval type-2 Gaussian fuzzy sets and genetic algorithms. IEEE Transactions on Fuzzy Systems 21(3), 412-425 (2013).
27. Jin, S., Diao, R., Quek, C., Shen, Q. Backward fuzzy rule interpolation. IEEE Transactions on Fuzzy Systems 22(6), 1682-1698 (2014).
28. Naik, N., Diao, R., Shen, Q.. Dynamic fuzzy rule interpolation and its application to intrusion detection. IEEE Transactions on Fuzzy Systems 26(4), 1878-1892 (2018).